Asian Journal of Chemistry; Vol. 27, No. 5 (2015), 1683-1691

ASIAN JOURNAL OF CHEMISTRY

http://dx.doi.org/10.14233/ajchem.2015.17475

Rheology, Mechanical Properties and Non-Isothermal Crystallization Kinetics of Poly(trimethylene terephthalate)/Thermoplastic Polyester Elastomer Blends

YINGBIN LIU, CHANGYING SONG, JIAN WANG, YUQING BAI and MINGTAO RUN*

College of Chemistry & Environmental Science, Hebei University, Baoding 071002, P.R. China

*Corresponding author: Tel: +86 312 5079386; E-mail: lhbx@hbu.cn

Received: 25 February 2014; *Accepted*: 27 May 2014; *Published online*: 20 February 2015; AJC-16869

In order to toughen poly(trimethylene terephthalate) (PTT) material, thermoplastic polyester elastomer (TPEE) was blended with PTT for preparing polymer blends and their rheology behaviors, phase morphology, impact strength dependence on molding temperatures, melting and non-isothermal crystallization kinetics were investigated by capillary rheometer, impact tester, scanning electron microscopy, wide angle X-ray diffraction and differential scanning calorimetry, respectively. The results suggest that the blends' apparent viscosities and the pseudoplasticity increase with increasing TPEE contents and TPEE has a good effect on improving the blends' melt viscosity. Thermoplastic polyester elastomer, which is partially miscible with PTT, also has a good toughening effect on PTT for the toughness increases with increasing TPEE content. However, the toughness decreases with molding temperatures increasing from 25 to 75 °C. The blends crystallize at lower rate and lower dimension than those of PTT. With increasing flexible TPEE, the blends show less crystallization ability for their more positive crystallization effective activation energy.

Keywords: Poly(trimethylene terephthalate), Thermoplastic polyester elastomer, Crystallization, Toughening, Miscibility.

INTRODUCTION

Compared to the familiar polyesters, such as poly(butylene terephthalate) (PBT), poly(ethylene terephthalate) (PET) and poly(ethylene 2,6-naphthalate) (PEN), poly(trimethylene terephthalate) (PTT) has a strong competitive due to its excellent properties (**Scheme-I**). These include good tensile strength, outstanding elastic recovery and dyeability, which make it an ideal candidate for applications in textile fiber, carpet and engineering plastic[1,2]. As an potential engineering thermoplastic material, PTT still has some shortcomings, such as poor impact resistance at lower temperatures, low melt viscosity, narrow processing temperatures when used as injection molding material; thereby, many research works have been reported for reinforcing or toughening of PTT[3-9].

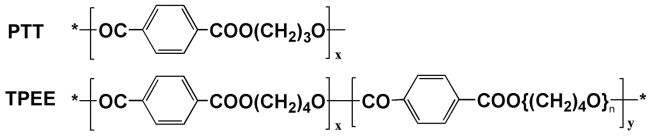

Scheme-I: Molecular formula of poly(trimethylene terephthalate) (PTT) and thermoplastic polyester elastomer (TPEE)

Polymer blending is a good method for producing new polymeric materials with desirable properties without having to synthesize a totally new material. Other advantages of polymer blending are versatility, simplicity and inexpensiveness. Due to the similarity in the chemical structure of above linear aromatic polyesters, numerous research works related to various aspects of polyesters' blends are available in literature. These include PTT/PBT[10-13], PTT/PET[14-16], PTT/polycarbonate[17,18], PTT/acrylonitrile-butadiene-styrene[19,20], PTT/PEN[21], PTT/polystyrene[22], PTT/PEO[23], PTT/ethylene propylene diene monomer copolymer/metallocene polyethylene[24] and so on. In these works, some of the properties of PTT were improved, such as the toughness[19,20,24], but the miscibility between the components is a key problem, which should be further resolved by using more proper polymers as modifying agents.

Thermoplastic polyester elastomers are block copolymers containing hard polyester segments and soft polyether segments[25-28] (**Scheme-I**). In TPEE, both polyether segments and uncrystallized polyester form amorphous parts, while some of the hard polyester segments form crystals and the crystals play the role of physical cross-linking points. Thermoplastic polyester elastomer has good flexibility, high melt stability and low melt viscosity, therefore it can be used to improve the impact strength and flexibility at high or low temperature of other polymers, such as polyoxymethylene, PBT, PET, *etc*. We proposed that TPEE could be used to toughen PTT as well as increasing PTT's melt viscosity.

Accordingly, the objectives of the present work are to investigate the influences of TPEE on the properties of PTT. Some PTT/TPEE blends were prepared and their rheological behaviours, phase morphology, impact strength and the non-isothermal crystallization kinetics were studied in detail. It should be noted that the amount of TPEE is in the range of 5-20 % for modifying PTT matrix.

EXPERIMENTAL

Poly(trimethylene terephthalate) (PTT) homopolymer was supplied in pellet form by Shell Chemicals (USA) with an intrinsic viscosity of 0.92 dL/g (M_w = 54,200 g/mol) measured in a phenol/tetrachloroethane solution (50/50, w/w) at 25 °C. Thermoplastic polyester elastomer (CH7563), supplied in pellet form by Sichuan Sunshine Plastics Co. (China), is a random multiblock copolymer of poly(butylene terephthalate) (PBT, 75 mol %) and poly(tetramethylene glycol) (PTMG, 25 mol %) and the average molecular weights of the PBT block and the PTMG block were 652 and 2070 and the intrinsic viscosity of 1.62 dL/g (M_w = 96,600 g/mol) measured in a phenol/tetrachloroethane solution (50/50, w/w) at 25 °C.

Blends preparation: Poly(trimethylene terephthalate) and TPEE were dried in a vacuum oven at 100 °C for 12 h before preparing the blends. Poly(trimethylene terephthalate) and TPEE were mixed together with different weight ratios of PTT/TPEE as follows: **A0**: 100/0; **A5**: 95/5; **A10**: 90/10; **A20**: 80/20; **A100**: 0/100 and then melt-blended in a SHJ-20 type, co-rotating twin-screw extruder with five heating sections, made by Nanjing Giant Machinery Co. (China), operating at a screw speed of 70 rpm and with temperatures of 210, 235, 250, 250, 250, 245 °C from the first section to the die. In order to depress the transesterification reactions or get the same transesterification extent between PTT and TPEE, the melt-blended process was less than 3 min[29,30] before the extruded resultant blend ribbons were cooled in cold water, cut up and re-dried before being used in measurements.

Rheology characterizations: The rheological measurements were performed on a XLY-II type capillary rheometer (Jilin University, China) with a capillary length of 40 mm and a diameter of 1 mm, respectively. The 1.2 g sample was put into the capillary at thermostatic temperature, held for 5 min and then measured at the pressure range of 6.1-73.5 kPa at 240 °C. The melt apparent viscosity, η_a, was defined by the Hagen-Poiseuille equation[24].

Characterization of phase morphology: The dried blend ribbons were cooled in liquid nitrogen and then fractured by impact stress. The phase morphology of the fracture surface, coated with a thin layer of gold, was investigated using a KYKY-2800B type Scanning Electron Microscope (KYKY Technology Development Ltd., China) at a voltage of 25 kV.

Dynamic mechanical characterization: Dynamic mechanical properties of the TPEE and PTT/TPEE blends were investigated using a dynamic mechanical analyzer (DMA, DMA-8000, Perkin-Elmer Co., USA). The temperature scans were carried out from -80 to 100 °C using a single-cantilever vibration mode at a constant heating rate of 2 °C/min and a frequency of 1 Hz. The blend pellets were made into the standard rectangular bar with size of 15 mm × 5 mm × 2 mm using a micro-injection molding machine (SZ-15, Wuhan Ruiming Machinery, China) with a cylinder temperature of 250 °C and mold temperature of 20 °C.

Wide-angle X-ray diffraction characterization: The wafers with size of 25 mm × 2 mm were prepared by using also the SZ-15 micro-injection molding machine with the cylinder temperature of 250 °C and mold temperatures of 25, 50 and 75 °C, respectively. Wide-angle X-ray diffraction (WAXD) curves were recorded on a D8 Advance type diffractometer system (Bruker, Germany) for the molded samples. Nickel-filtered CuK_α (λ = 0.15418 nm) radiation generated at 40 kV and 40 mA was used. The diffraction curves were recorded from 2θ scans in the range of 5-60º at a scanning speed of 10 º/min using a step size of 0.02°.

Mechanical properties testing: The normative rectangular bars used in mechanical properties testing were all prepared by the above micro-injection molding machine at the cylinder temperature of 250 °C and specific mold temperatures of 25, 50 and 75 °C (electrical heated and controlled by computer at room temperature of 14 °C). The notched charpy impact tests were carried out according to the ISO 179-1982 standard using samples with splines and an impact tester (JJ-20, Changchun Intelligent Instrument Co. Ltd., China); the data reported were the mean and standard deviation from five determinations.

Differential scanning calorimetry studies: The melting behaviours were performed on a Perkin-Elmer Diamond type DSC instrument (USA), which was calibrated with indium as the standard substance prior to use; the weights of the samples were approximately 6 mg. The dried samples were heated to 255 °C under nitrogen atmosphere, held for 5 min and then quickly quenched to -40 °C under a cooling rate of 100 °C/min (the fastest cooling rate of the DSC used, in order to get more amorphous phase), then held at -40 °C for 3 min; subsequently the glass transition temperature (T_g), cold-crystallization temperature (T_{cc}) and melting point temperature (T_m) were measured by secondly heating the sample to 255 °C at a heating rate of 10 °C/min; the second melting process was recorded.

The non-isothermal crystallization behaviours were also performed on the DSC. The sample was heated to 255 °C in nitrogen, held for 5 min and then cooled to 30 °C at constant cooling rates of 10, 15, 20 and 25 °C/min, respectively. The exothermic curves of heat flow as a function of temperature were recorded and investigated.

In order to study the influences of the molding temperatures on the crystallization behaviours of the blends, the melting behaviours of the samples as-molded at different temperatures were measured by DSC. They were heated from 20 to 255 °C at a heating rate of 10 °C/min and the heating process was recorded.

RESULTS AND DISCUSSION

Rheological behaviours: Fig. 1 shows the rheological curves of different melts at 240 °C in the form of the plot of apparent viscosity (η_a) *vs.* shearing rate. The results show that all the melts are pseudo-plastic fluids for the apparent viscosity decreases greatly with increasing shear rate. A100 has the

largest apparent viscosity because of its higher M_w (9.66×10^4) than that of **A0** (5.42×10^4), which leads to more molecular chain entanglements in the melt. Therefore, TPEE's melt has the strongest sensitivity to shearing rate among all the samples in low shearing rates because of the unentanglements of molecular chains; even its apparent viscosity is lower than those of the blends as shearing rate is larger than 400 s^{-1} due to the further unentanglements of the molecular chains. Poly(trimethylene terephthalate) has the lowest apparent viscosity and the η_a decreases slowly with increasing shearing rate because of its relative rigid molecular chains, which are not sensitive to shearing rate. While for the blends (**A5**, **A10**, **A20**), their apparent viscosities decrease slowly with increasing shearing rate and increase with increasing TPEE contents. Therefore, the increasing viscosity may be favorable for improving the processing property of PTT by adding more than 5 % TPEE. The Non-Newtonian index was calculated and its relationship with TPEE contents is shown in Fig. 2. It can be seen that $n < 1$ and it decreases with increasing TPEE content. This result suggests that the pseudoplasticity increases slightly with increasing TPEE content.

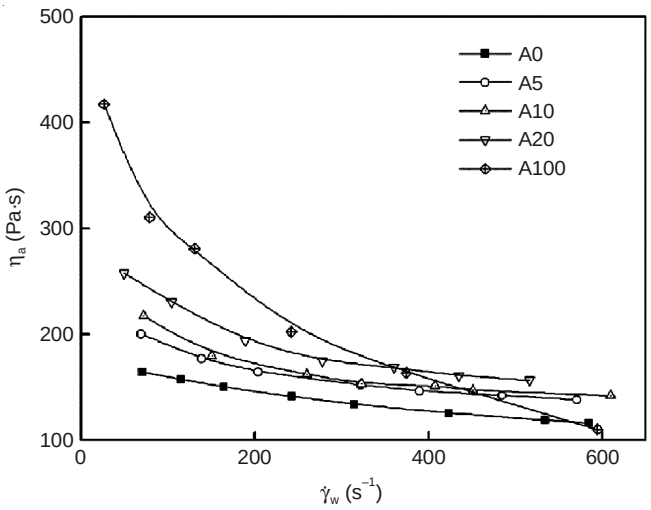

Fig.1. Relationship between η_a and $\dot{\gamma}_w$ of the various samples

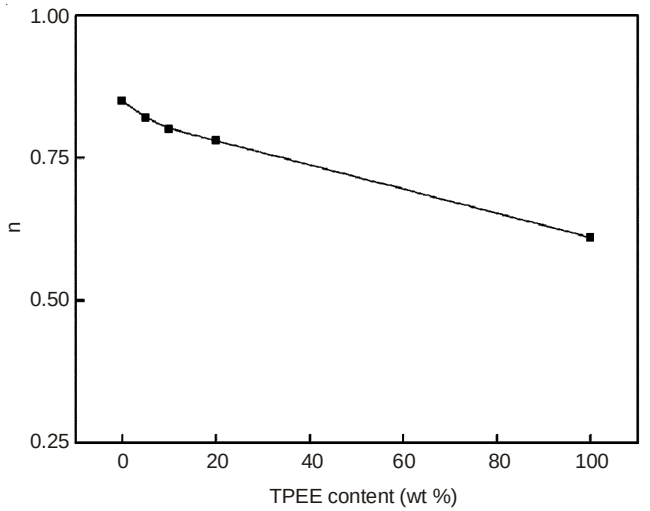

Fig. 2. Relationship between n and thermoplastic polyester elastomer (TPEE) contents

Morphology and miscibility analysis: For a semicrystalline polymer, the introduction of a second component may induce changes in the arrangement and the state of molecular chains, intermolecular interactions and phase morphology, which will affect their crystallization and melting behaviours, in which the miscibility of two components is a key issue.

Fig. 3 exhibits SEM images of fracture surfaces of different blends. In Fig. 3a, for **A0**, the fracture surface is not smooth but many parallel folds were observed (parallel to the arrow of the impact direction), so **A0** was brittle at low temperature (≤ 100 °C). For the blends, the fracture surfaces are more irregular and rough, indicating that they were ductile fractures and their toughness was better than that of **A0** (Fig. 3b-d). On the other hand, with the low magnification in Fig. 3b-d, we could not find significant, large dispersed phase particles in the fracture surface. With a four times larger magnification, as shown in Fig. 3e of **A20**, only a few small dispersed particles, with size smaller than 2 mm, were observed in the matrix and the interface between the particles and the matrix is obscure. This result indicates that PTT and TPEE were at least partially miscible in the blends. As shown in **Scheme-I**, the similar chemical structure between PTT and the rigid block of TPEE is maybe the reason of miscibility. As reported earlier[7,9,19,23,24], some vinyl elastomers (dispersed phase) were often shown with much bigger phase size in PTT matrix than this TPEE phase, thus, we believe that TPEE has better miscibility with PTT than those virgin vinyl elastomers.

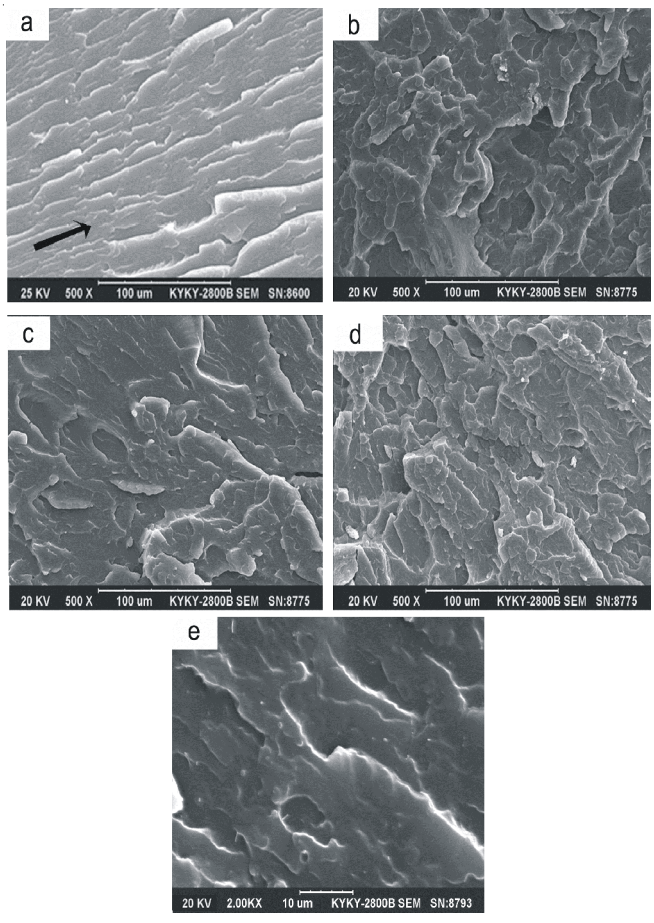

Fig. 3. SEM micrographs of the various samples; (a) A0 × 500; (b) A5 × 500; (c) A10 × 500; (d) A20 × 500; (e) A20 × 2000

The miscibility of two components is also usually discussed in terms of the appearance of either single or double T_gs[31]. Fig. 4 shows the DSC heating scans for different samples and the thermodynamic parameters are shown in Table-1. In Fig. 4, the T_gs of **A0** and **A100** are 43.1 and 15.8 °C, respectively and each blend's curve shows a single T_g in the temperature range of -30 to 50 °C that depends on the composition, which shifts monotonically to lower temperatures with increasing TPEE content. According to the reports made on PTT/PBT blends[10-13], this system was proved to be completely miscible evident from a unique glass transition temperature which increased upon addition of PTT content. In multiblock TPEE molecules, because 75 % (mole ratio) chain blocks is PBT blocks; it can be deduced that PTT is miscible with these PBT blocks of TPEE. Therefore, it is believed that PTT and TPEE components are, at least, partially miscible in the amorphous state.

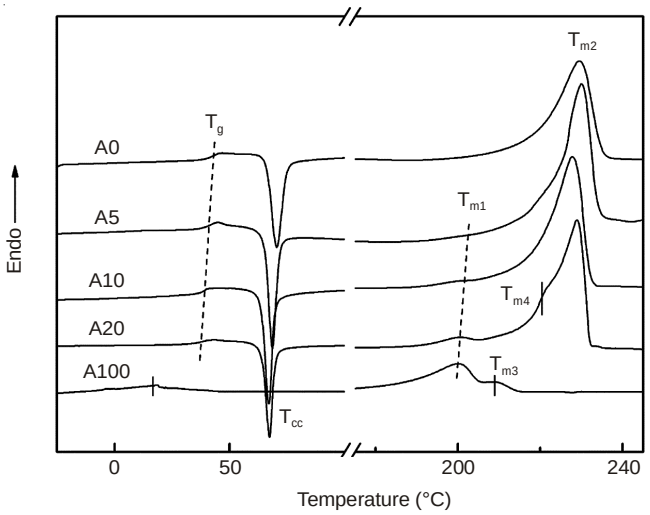

Fig. 4. Differential scanning calorimetry heating curves of the various samples

In order to further determining the T_gs of these materials, DMA tests were carried out. As shown in Fig. 5, the tan δ *vs*. temperature curve of **A100** is shown with a wide and weak peak in the temperature range of -45 to 60 °C with a maximum value at about 15.6 °C. This result consists with that observed in the DSC curve of **A100**. It is known that TPEE is a copolymer of poly(butylene terephthalate)-poly(tetramethylene glycol), in which poly(butylene terephthalate) rigid block must has higher T_g and poly(tetramethylene glycol) soft block must has a lower T_g. However, the DMA result of TPEE suggests that the glass transitions of both blocks are overlapped, therefore, only one weak glass transition behaviour in wide temperature range can be seen for **A100**. For **A0** (PTT), a sharp tan δ peak (T_g) was observed at about 51.2 °C. For the **A5-A20** blends, the tan δ peaks (T_g) were observed at 51.2, 48.2 and 46.5 °C, respectively. These results suggest that T_g of the blends decreases with increasing TPEE content. Therefore, judging from the results of the DSC, DMA and SEM, PTT and TPEE were at least partially miscible in blends.

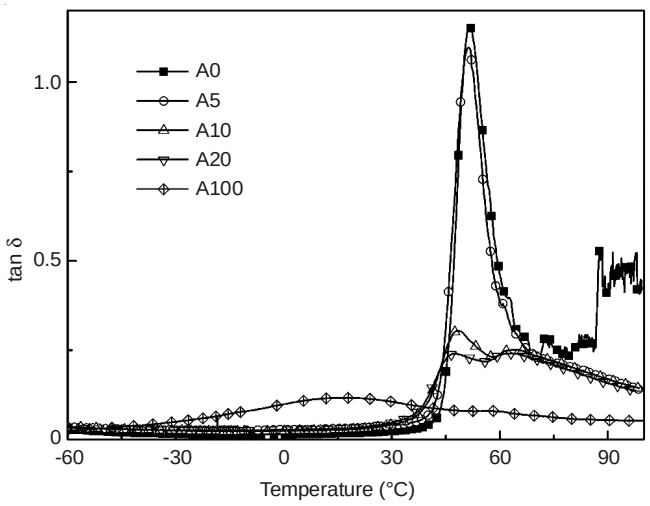

Fig. 5. Curves of tan δ *vs*. temperature of the various samples

The cold-crystallization behaviours of **A0** and the blends during the heating scans were also observed in the temperature range of 50 to 80 °C. The cold-crystallization temperatures (T_{cc}) and exothermal enthalpy (ΔH_{cc}) of different blends decreased with increasing TPEE content. Because TPEE has softer polymer chain blocks than those of PTT, these soft chains facilitate the motions of PTT chains towards the growing crystals by reducing the energy barrier for the transport of the PTT chain segments. The composition dependent behaviour of T_{cc} and ΔH_{cc} in the blends can also be taken as a further evidence for partial miscibility. The cold-crystallization behaviour was not observed in **A100**, which maybe because of two reasons: (1) in the multiblocks macromolecules, some of the rigid polyester blocks has crystallized in former quenched process; and (2) the other amorphous rigid polyester blocks could not cold-crystallize in this heating process due to the limitations of the connected soft PTMG blocks or the crystallized phase.

In Fig. 4, the melting point (T_m) of **A0** is 229.3 °C (T_{m2}) and **A100** had two melting peaks of 200.8 °C (T_{m1}) and 209.1 °C (T_{m3}). Although TPEE was quenched from the melt, some crystals might have formed during the quenching process because of the fast crystallization ability of the rigid polyester blocks in

TABLE-1
DIFFERENTIAL SCANNING CALORIMETRY PARAMETERS OF PTT/TPEE BLENDS IN HEATING PROCESS

Sample	T_g (°C)	T_{cc}[a] (°C)	ΔH_{cc}[b] (J/g)	T_{m1} (°C)	T_{m2} (°C)	T_{m3} (°C)	T_{m4} (°C)	ΔH_m[c] (J/g)
A0	43.1	70.3	-20.1	—	229.3	—	—	48.3
A5	41.0	68.5	-16.5	—	230.1	—	—	45.5
A10	38.8	67.2	-19.2	201.3	227.7	—	—	44.6
A20	37.9	67.1	-14.4	200.8	229.4	—	220.9	43.8
A100	15.8	—	—	200.4	200.8	209.1	—	30.4

[a]peak temperature of the cold-crystallization curve; [b]exothermic enthalpy of the cold-crystallization; [c]the total endothermic enthalpy of melting peaks including peaks of T_{m1}, T_{m2}, T_{m3}, T_{m4}; PTT: poly(trimethylene terephthalate); TPPE: thermoplastic polyester elastomer

the TPEE copolymer. The double melting points phenomenon of TPEE is perhaps due to the melting of the different crystals with different sizes or dimensions. For the three blends **A5**, **A10** and **A20**, as the TPEE content increases from 5 to 20 %, the intensity of the melting peak T_{m1} attributed to TPEE increases gradually; while the values of the T_{m2} attributed to PTT component, also slightly decreases except for that of **A20**. The melting point depression behaviour was also reported as well in the blends of PTT/PBT[10] and it was taken as an evidence for the partially miscible of PTT and TPEE. For **A20**, double melting peaks, T_{m2} (229.4 °C) and T_{m4} (220.9 °C), were observed in its DSC curve, which may be because of the influence of TPEE component. When TPEE content increases to 20 %, two types of crystals with different sizes or dimensions form in the blend, so it show double melting peaks. Moreover, ΔH_m values calculated from both the melting enthalpy of PTT and TPEE also decreases with increasing TPEE content. The changes of the ΔH_m can also be taken as a further evidence for partially miscibility of PTT with TPEE.

Non-isothermal crystallization kinetics analysis: The relative crystallization (X_t) as a function of temperature is defined by the following equation:

$$X_t = \frac{\int_{t_0}^{t}(dH/dt)dt}{\int_{t_0}^{t_\infty}(dH/dt)dt} = \frac{A_t}{A_\infty} \quad (1)$$

where dH/dt is the rate of heat evolution, t_0 and t_∞ are the time at which crystallization starts and ends, respectively; and A_t and A_∞ are areas under the normalized DSC curves at time t and the end of the crystallization, respectively. The relationship between temperature T and time t during the non-isothermal crystallization process is given by eqn. (2), as follows:

$$t = \frac{|T_0 - T|}{D} \quad (2)$$

where t is the crystallization time after t_0, T_0 is the temperature at which crystallization begins (t = 0), T is the temperature at a crystallization time t and D is the cooling rate.

The non-isothermal crystallization exothermic peaks of **A0** and **A5** blends (the curves of A10 and A20 are similar to **A5** and are omitted) at various cooling rates are shown in Fig. 6a,b. In Fig. 6, the exothermic peak temperature (T_{cp}) shifts to lower temperature with increasing cooling rate from 10 to 25 °C/min; *e.g.*, T_{cp} of **A0**, **A5**, **A10** and **A20** shifted 9.5, 7.2, 6.4 and 6.3 °C, respectively. These results indicate that the greater the content of TPEE in the blend, the less the influence of the cooling rate on the crystallization.

From the DSC digital information and eqn. 1, the relative crystallinity (X_t) can be calculated at different temperatures. Since the non-isothermal crystallization is a rate-dependent process, Ozawa[32] took into account the effect of cooling (or heating) rate, D, on the crystallization process from the melt or glassy state and modified the Avrami equation as follows:

$$1 - X_t = \exp\left(-\frac{K(T)}{|D|^m}\right) \quad (3)$$

$$\log[-\ln(1 - X_t)] = \log K(T) - m \log|D| \quad (4)$$

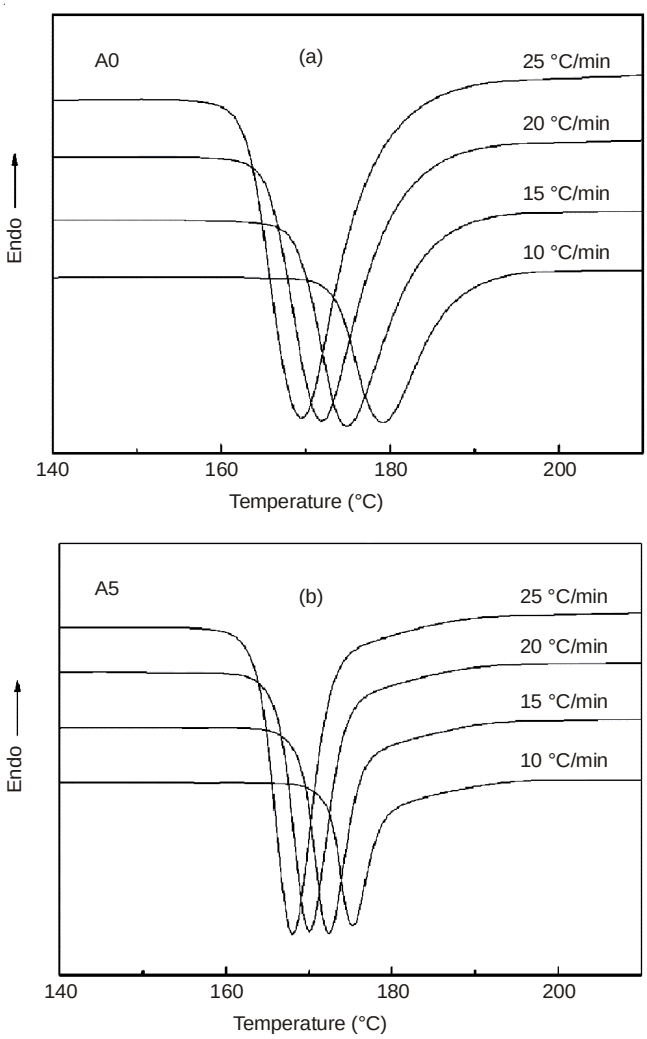

Fig. 6. Differential scanning calorimetry cooling curves of (a) A0 and (b) A5 samples at various cooling rates

where K(T) is a function related to the overall crystallization rate that indicates how fast crystallization proceeds and m is the Ozawa exponent that depends on the dimension of crystals growth. According to the Ozawa's theory and plots of log [-ln(1-X_t)] *versus* log |D| at a given temperature, a series of straight lines will be obtained if Ozawa analysis is valid and the crystallization kinetic parameters and can be derived from the slope and the intercept, respectively.

The results of the Ozawa analysis for A0 and A5 samples are shown in Fig. 7a,b and a series of straight lines are obtained and the values of m and log K(T) are calculated and shown in Fig. 8a,b. The values of m and log K(T) of the various blends are different with decreasing temperatures,

In Fig. 8a, for **A0**, the curve of m decreases much first as temperature decreases from 190 to 182 °C then levels off as temperature decreases from 180 to 170 °C, *i.e.* it decreases from 3.4 to about 2.5 with decreasing temperatures, indicating that PTT's nucleation dimensions change from three-dimensional at high temperatures to two-dimensional at low temperatures[6]. For **A5** blend, the curve of m firstly decreases gradually as temperature decreases from 190 to 182 °C and then increases much as temperature decreases from 180 to 170 °C, *i.e.*, it first decreases from 2 to about 1.7 and then increases to 3. This result suggest that the nucleation dimensions of the blend **A5**

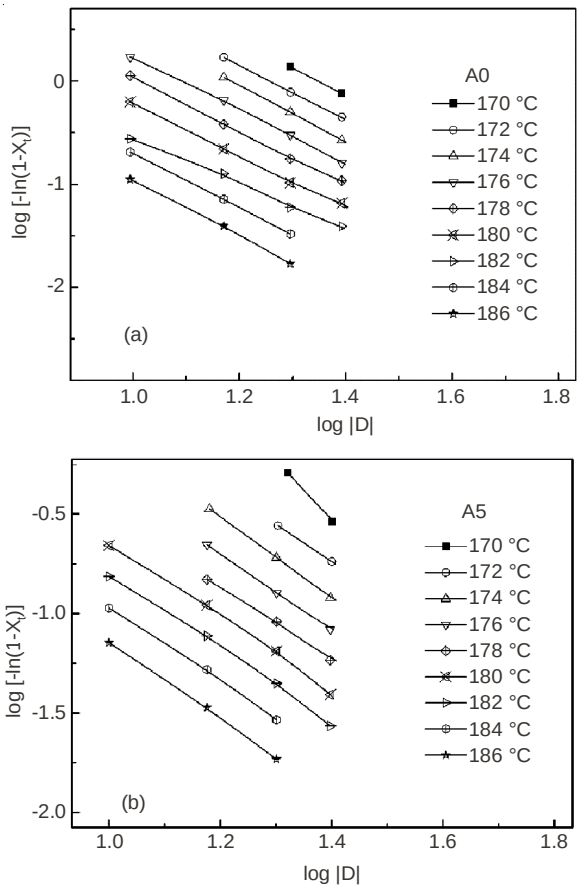

Fig.7. Ozawa plots of log [-ln(1-X_t)] *vs.* log |D| for (a) A0 and (b) A5 samples

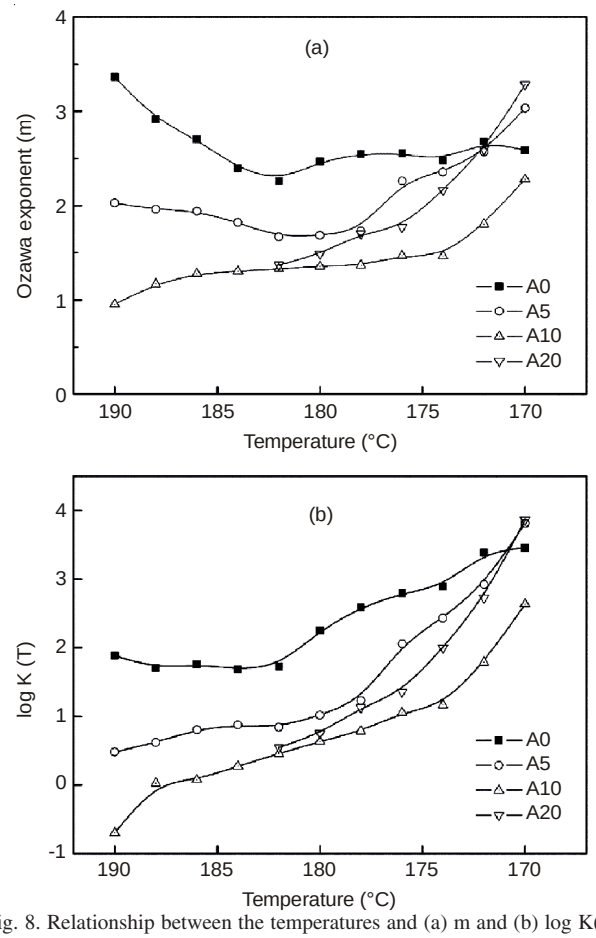

Fig. 8. Relationship between the temperatures and (a) m and (b) log K(T)

change from two-dimensional at high temperatures to three-dimensional at low temperatures. For **A10** and **A20** blends, the curves of m increase with decreasing temperatures, which are different to those of **A0** and **A5** and their values increase from 1.0 to 2.4 for **A10** while from 1.4 to 3 for **A20**, indicating that the nucleation dimensions change from one-dimensional to three-dimensional with decreasing temperatures. It should be noted that the m values of **A20** are higher than those of **A10**, *i.e.* the nucleation dimensions in **A20** are larger than those in **A10** as temperatures are lower than 180 °C, indicating that the flexible TPEE may improve the three-dimensional nucleation of PTT especially at lower temperatures.

In Fig. 8b, log K(T) values are nearly unchanged as temperatures decrease from 190 to 182 °C, while they increase gradually with decreasing temperatures from 180 to 170 °C. For **A5**, **A10** and **A20** blends, log K(T) values first increase gradually and then increase rapidly with decreasing temperatures. Compared the log K(T) of **A0** with those of the blends, **A0** has much higher crystallization rate than those of the blends especially at high temperatures (190-178 °C). For the various blends, the crystallization rates of **A10** are smaller than those of **A5**, but those of **A20** are larger than those of **A10**, indicating that the blends' crystallization rate is dependent on TPEE contents. It should be noted that the log K(T) of **A5** and **A20** at 170 °C were even larger than that of **A0**, suggesting that at low temperatures, the blends have larger crystallization rate.

Crystallization effective activation energy: In order to obtain the reliable values of the effective activation energy on the melt cooling process, Friedman[33] and Vyazovkin *et al.*[34-36] developed different methods, respectively. In this paper, the Friedman analysis is carried out by first differentiating the X_t function with respect to time to obtain the instantaneous crystallization rate as a function of time $\tilde{X}_t$. The Friedman equation is expressed as:

$$\ln(\tilde{X}_t) = B - \frac{\Delta E}{RT} \quad (5)$$

where $\tilde{X}_t$ is the instantaneous crystallization rate as a function of time at a given conversion X_t, B is an arbitrary pre-exponential parameter and is the crystallization effective activation energy at a given conversion X_t. A plot according to eqn. 5 can then be performed for various values of relative crystallinity using the data obtained from both $\tilde{X}_t$ and X_t functions and the crystallization energy of the non-isothermal crystallization process for a given relative melt conversion X_t can finally be estimated from the slope of the plot.

Fig. 9 gives the effective energy for **A0** and various blends. It can be seen that the E_a values of **A0** show apparently different changes with those blends. For **A0**, E_a increases with increasing $\tilde{X}_t$, indicating that the crystallization of PTT becomes difficult as the crystallization proceed. However, for **A5-A20** blends, E_a decreases first and then slightly increases with increasing $\tilde{X}_t$ and their values of E_a are much positive than that of **A0**, especially at lower $\tilde{X}_t$. The changing trends of E_a for the blends suggest that it is difficult for the blends to crystallize at the beginning of the crystallization ($\tilde{X}_t$ = 0.1), while it becomes easier as the crystallization increases ($\tilde{X}_t$ = 0.1-0.5). At lower $\tilde{X}_t$ stage (such as 0.1, it means at high temperatures in the cooling process), the blend is difficult to start crystalli-

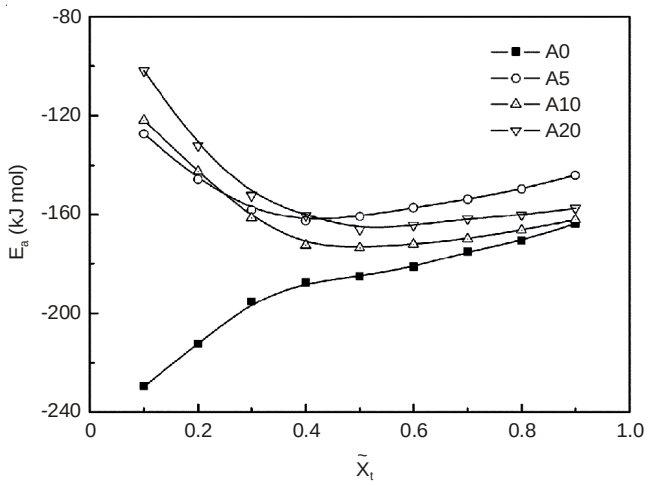

Fig. 9. Friedman plots of $\tilde{X}_t$ *vs.* ΔE for various samples 10

zation because of the counteract of TPEE molecules which is so active at high temperatures; while with the decreasing of the temperature, TPEE molecules become less active and it can be also served as nucleus for the crystallization of PTT, so E_a decreases with increasing $\tilde{X}_t$ ($\tilde{X}_t$ = 0.1-0.5). When $\tilde{X}_t$ is larger than 0.5 (at the same time the sample's temperature becomes low), the crystallization becomes a little difficult (E_a increases slightly) because of the low active molecules at low temperature.

Influence of molding temperatures on impact strength: In order to study the relationship between molding temperatures and material properties, we studied the influences of the various molding temperatures on the impact strength (σ_i) of the injection molded samples (Table-2). Firstly, at each molding temperature, such as at 25 °C, σ_i values increase with increasing TPEE content, suggesting that TPEE has a good toughening effect on PTT material. Secondly, σ_i gradually decreases with increasing molding temperatures, *i.e.*, the samples molded at 25 °C have the largest σ_i values. It is believed that the changing of σ_i is relative to the sample's crystallinity. Generally, the semicrystalline polymer form larger crystallinity at higher molding temperatures compared those at lower temperatures. As a result, the decreasing of the impact strength will occur.

The T_gs of PTT and TPEE are 43.1 and 15.8 °C, respectively (Table-1), thus as molding temperature is 25 °C, TPEE can crystallize but PTT can't crystallize or only form some crystal nucleus. However, at 50 °C, PTT may crystallize a few for 50 °C is only a little higher than 43.1 °C, while TPEE can crystallize more for 50 °C is much higher than 15.8 °C; at 75 °C, both TPEE and PTT can crystallize much for their molecular chains are more active than those at 25 and 50 °C. Therefore, it is believed that PTT/TPEE blends will have larger crystallinity at higher molding temperatures. In order to verify the above presumptions, the DSC and X-ray measurements were performed and shown in Figs. 10 and 11 and the parameters are also listed in Table-2.

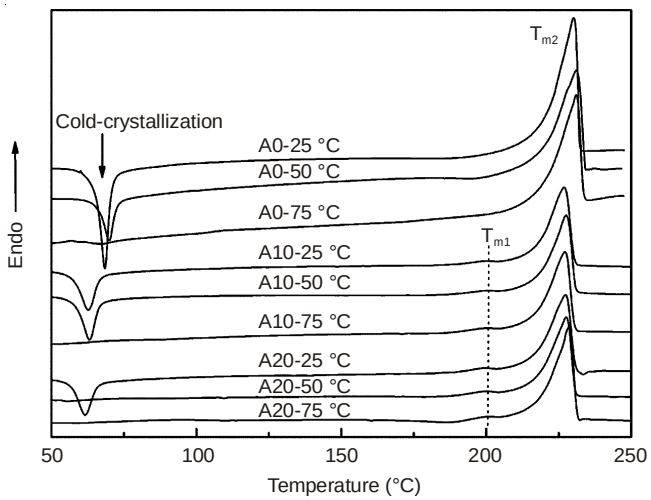

Fig. 10. Differential scanning calorimetry heating curves of the various samples after molded at different temperatures

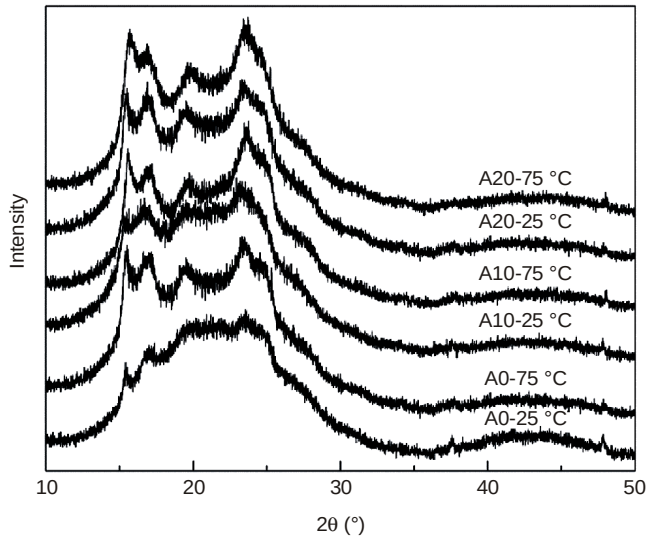

Fig. 11. WAXD curves of the various samples after molded at different temperatures

Fig. 10 shows the DSC melting curves of the as-molded samples at different molding temperatures. It can be seen that the sample **A0** first cold-crystallized and then melted at 229.3 °C and the cold-crystallization peak intensity became weak with increasing molding temperatures from 25 to 75 °C; At

TABLE-2
EFFECT OF MOLDING TEMPERATURES ON THE TOUGHNESS OF PTT/TPEE BLENDS

T (°C)	A0			A10			A20		
	σ_I (kJ/m^2)	ΔH_t^a (J/g)	X_{WAXD}^b (%)	σ_I (kJ/m^2)	ΔH_t^a (J/g)	X_{WAXD}^b (%)	σ_I (kJ/m^2)	ΔH_t^a (J/g)	X_{WAXD}^b (%)
25	5.53 ± 0.1	36.6	31.2	7.41 ± 0.2	44.7	34.5	7.69 ± 0.2	52.7	38.7
50	5.32 ± 0.1	41.5	38.5	7.23 ± 0.2	46.1	39.2	7.50 ± 0.2	55.1	40.5
75	4.96 ± 0.1	67.2	46.2	7.04 ± 0.1	61.9	44.8	7.32 ± 0.1	61.2	41.2

[a]melting enthalpy of the crystals formed in molding process; [b]relative crystallinity calculated from WAXD curves; PTT: poly(trimethylene terephthalate); TPPE: thermoplastic polyester elastomer

25 and 50 °C, sample **A10** first cold-crystallized and then melted with two melting points (T_{m1} and T_{m2}) corresponding to the melting of TPEE and PTT components respectively. For **A20**, it cold-crystallized at 25 °C giving out much enthalpy and at 50 °C giving out only a few enthalpy; but at 75 °C, A10 and **A20** didn't cold-crystallized. The non-cold crystallization phenomena must be due to their high crystallinity that had formed in the molding process. The total enthalpy (ΔH_t) in the molding process is calculated by the following eqn. 6

$$\Delta H_t = \Delta H_m - \Delta H_{cc} \quad (6)$$

where ΔH_m is the melting enthalpy of the two melting peaks (T_{m1} and T_{m2}), ΔH_{cc} is the exothermal enthalpy in cold-crystallization. ΔH_t means the amount of melting enthalpy of the crystals that form in the molding process. It can be seen in Table-2 that ΔH_t values increase with increasing molding temperatures, especially at 75 °C. This result suggested that the blends of PTT/TPEE can crystallize with more crystallinity at higher molding temperatures.

Fig. 11 shows the WAXD curves of **A0-A20** at different molding temperatures. In Fig. 11, several strong reflections peaks in each curve (at around 15.6, 17.0, 19.6, 23.7 and 25.2°) are observed and their crystal lattice is also designated, which are the specific reflections of PTT[37]. It should be noted that no other separated diffraction peaks are observed in these curves, indicating that only the crystal structure of PTT formed in the blends can be detected, although TPEE can crystallize, which maybe because of the low crystal content of TPEE in blends and its diffraction peaks are overlapped by those of PTT. The diffraction peak area was integrated by using the testing software of the instrument and the crystallinity of each blend was also calculated according to their components ratio by using the following formula,

$$X_{WAXD} = \frac{A_c}{A_c + A_a} \times 100\ \% \quad (7)$$

where X_{WAXD} is the relative crystallinity, A_c and A_a are the diffraction area of the crystalline phase and the amorphous phase divided from the WAXD curve, respectively. The calculated X_{WAXD} values are also listed in Table-2. It can be seen that X_{WAXD} increases with increasing molding temperatures. Therefore, it is presumed that the declined toughness of the samples is due to their increasing crystallinity with increasing molding temperatures. Furthermore, compared the ΔH and X_{WAXD} of **A0**, with those of **A10** and **A20** at the same molding temperature, it can be found that (1) at 25 and 50 °C, they increase with the increasing TPEE content and (2) at 75 °C, they decrease with increasing TPEE content. When molding temperatures are 25 and 50 °C, PTT's molecular chain segments are not active but TPEE's molecular chain segments are active and TPEE will improve the cold-crystallization of PTT in the blends since the more flexible polymer chains facilitates the motions of the crystallizable chains towards the growing crystals, by reducing the energy barrier for the transport of the crystallizable segments[38]. Therefore, the crystallinity increases although PTT's contents decrease from 100 to 80 %. However, when the molding temperature is 75 °C, both PTT and TPEE's molecular chain segments are active, so the crystallinity is predominantly related to the content of PTT and it decreases with increasing TPEE content.

Moreover, Table-2 showed that σ_i increases much with increasing TPEE content, suggesting that TPEE has a good toughening effect on PTT because of TPEE's good flexibility of the molecular chains.

Conclusion

In the blends of PTT and TPEE, TPEE cannot only act as a toughening agent for PTT material but can also improve the processing viscosity of PTT. The non-isothermal crystallization kinetics studies suggest that the blends have lower crystallization rate and spherulite dimensions than those of PTT. The blends have much higher crystallization activation energy than pure PTT. The molding temperature has great influence on the impact strength of the blends, *i.e.* the resultant blends have large impact strength at low molding temperatures (25 °C) for their low crystallinity.

ACKNOWLEDGEMENTS

This work is supported by the Natural Science Foundation of Hebei Province (B2010000219).

REFERENCES

1. J.L. Zhang, *J. Appl. Polym. Sci*., **91**, 1657 (2004).
2. N. Apiwanthanakorn, P. Supaphol and M. Nithitanakul, *Polym. Test*., **23**, 817 (2004).
3. F.C. Chiu, H.Y. Lee and Y.H. Wang, *J. Appl. Polym. Sci*., **107**, 3831 (2008).
4. A. Romo-Uribe, B. Alvarado-Tenorio, M.E. Romero-Guzmán, L. Rejón and R. Saldivar-Guerrero, *Polym. Adv. Technol*., **20**, 759 (2009).
5. I. González, J.I. Eguiazábal and J. Nazábal, *J. Appl. Polym. Sci*., **102**, 3246 (2006).
6. M.T. Run, H.Z. Song, C.G. Yao and Y.J. Wang, *J. Appl. Polym. Sci*., **106**, 868 (2007).
7. S.H. Jafari, A. Yavari, A. Asadinezhad, H.A. Khonakdar and F. Böhme, *Polymer*, **46**, 5082 (2005).
8. Y.C. Shu and K.J. Hsiao, *J. Appl. Polym. Sci*., **106**, 644 (2007).
9. H.B. Ravikumar, C. Ranganathaiah, G.N. Kumaraswamy and S. Thomas, *Polymer*, **46**, 2372 (2005).
10. N. Dangseeyun, P. Supaphol and M. Nithitanakul, *Polym. Test*., **23**, 187 (2004).
11. P. Supaphol, N. Dangseeyun and P. Srimoaon, *Polym. Test*., **23**, 175 (2004).
12. Y.H. Kuo and E.M. Woo, *Polym. J*., **35**, 236 (2003).
13. G. Li, K. Wang, S. Li and Y. Shi, *J. Macromol. Sci*., **46**, 569 (2007).
14. H. Liang, F. Xie, B. Chen, F.Q. Guo, Z. Jin and F.S. Luo, *J. Appl. Polym. Sci*., **107**, 431 (2008).
15. M.T. Run, Y.P. Hao and C.G. Yao, *Thermochim. Acta*, **495**, 51 (2009).
16. H.J. Chiu, *Polym. Eng. Sci*., **47**, 2005 (2007).
17. A. Yavari, A. Asadinezhad, S.H. Jafari, H.A. Khonakdar, S. Ahmadian and F. Böhme, *Macromol. Mater. Eng*., **290**, 1091 (2005).
18. I. González, J.I. Eguiazábal and J. Nazábal, *J. Appl. Polym. Sci*., **108**, 3828 (2008).
19. M.L. Xue, Y.L. Yu, H.H. Chuah, J.M. Rhee and J.H. Lee, *J. Appl. Polym. Sci*., **108**, 3334 (2008).
20. W. Wang, M. Yao, H.S. Wang, X. Li and M.T. Run, *J. Macromol. Sci. Part B Phys*., **52**, 574 (2013).
21. M.T. Run, Y.J. Wang, C.G. Yao and H.C. Zhao, *J. Appl. Polym. Sci*., **103**, 3316 (2007).
22. J.M. Huang, *J. Appl. Polym. Sci*., **88**, 2247 (2003).
23. G. Guerrica-Echevarria, J.I. Eguiazábal and J. Nazábal, *Eur. Polym. J*., **43**, 1027 (2007).
24. M.T. Run, H.Z. Song, Y.J. Wang, C.G. Yao and J.G. Gao, *Front. Chem. Eng. China*, **1**, 238 (2007).
25. S.H. Cho, Y.J. Jang, D.M. Kim, T.Y. Lee, D.H. Lee and Y.K. Lee, *Polym. Eng. Sci*., **49**, 1456 (2009).

26. C.C. Li, D. Zhang and Z.Y. Li, *J. Appl. Polym. Sci*., **84**, 1716 (2002).
27. J.M. Lee, B.H. Choi, J.S. Moon and E.S. Lee, *Polym. Test*., **28**, 854 (2009).
28. G. Colomines, J.J. Robin, P. Notingher and B. Boutevin, *Eur. Polym. J*., **45**, 2413 (2009).
29. Y. Shi and S.A. Jabarin, *J. Appl. Polym. Sci*., **81**, 23 (2001).
30. A.M. Kenwright, S.K. Peace, R.W. Richards, A. Bunn and W.A. MacDonald, *Polymer*, **40**, 5851 (1999).
31. G. Guerrica-Echevarria, J.I. Eguiazábal and J. Nazábal, *J. Appl. Polym. Sci*., **92**, 1559 (2004).
32. T. Ozawa, *Polymer*, **12**, 150 (1971).
33. H.L. Friedman, *J. Polym. Sci. C*, **6**, 183 (1964).
34. S. Vyazovkin, *J. Comput. Chem*., **22**, 178 (2001).
35. S. Vyazovkin and N. Sbirrazzuoli, *Macromol. Rapid Commun*., **23**, 766 (2002).
36. S. Vyazovkin, A.K. Burnham, J.M. Criado, L.A. Pérez-Maqueda, C. Popescu and N. Sbirrazzuoli, *Thermochim. Acta*, **520**, 1 (2011).
37. S. Poulin-Dandurand, S. Perez, J.F. Revol and F. Brisse, *Polymer*, **20**, 419 (1979).
38. M.C. Righetti, M.L. Di Lorenzo, M. Angiuli, E. Tombari and P. La Pietra, *Eur. Polym. J*., **43**, 4726 (2007).